

# The Effect of Coatings on the Resistance Spot Welding Behavior of 780 MPa Dual-Phase Steel

*Both the hot-dipped galvanized and the galvanized steels exhibited similar welding behavior*

BY M. TUMULURU

**ABSTRACT.** Dual-phase steels are commercially available with hot-dipped galvanized (HDGA) or hot-dipped galvanized (HDGI) coatings. An investigation was undertaken to examine whether differences exist in the resistance spot welding behavior of 780 MPa dual-phase steel with HDGA coating compared to the one coated with HDGI coating. The resistance spot welding evaluations consisted of determining the welding current ranges for the steels with HDGA and HDGI coatings by determining the current required to obtain the minimum weld size and the current required to cause expulsion of weld metal. Shear-tension and cross-tension tests were performed on spot welds made on steels with both HDGA and HDGI coatings. Weld cross sections from both types of coatings were examined for weld quality. Weld microhardness profiles were determined to examine hardness variations across the welds. Cross sections of HDGA and HDGI coatings as well as the electrode tips after welding were examined using a scanning electron microscope. Composition profiles across the coating depths were analyzed using a glow-discharge optical emission spectrometer to understand the role of coating in resistance spot welding. Contact resistance was measured to examine its contribution to the current required for welding. The results indicated that 780 MPa dual-phase steel showed similar overall welding behavior with HDGA and HDGI coatings. Further, weld shear and cross-tension strengths were independent of the type of coating. The results of the study are presented along with a discussion of the structure and the role of coatings in welding. A brief discussion of the physical metallurgy of 780 MPa dual-phase steel is

presented to explain weld microstructural evolution.

## Introduction

Dual-phase steels are finding increased use in automotive bodies due to a combination of high strength and high ductility; hence, they possess excellent formability (Ref. 1). Dual-phase steel possesses a unique microstructure consisting of ferrite and martensite that offers high strength to these steels coupled with high formability. Due to these features, automotive companies are finding that the use of these steels can enable them to not only reduce overall weight of an automobile but, at the same time, offer improved crash protection to the vehicle occupants. Dual-phase steels are commercially available at present in 500, 590, 780, and 980 MPa minimum tensile strength levels. These steels are available with either a hot-dipped galvanized (HDGI) coating or a hot-dipped galvanized (HDGA) coating.

Two types of coatings are generally applied to steel sheets used in the automotive industry, namely galvanized and galvanized coatings. Galvanized coatings contain essentially pure zinc with about 0.3 to 0.6 wt-% aluminum. The term "galvanized" comes from the galvanic protec-

tion that zinc provides to steel substrate when exposed to a corroding medium. A galvanized coating is obtained by additional heating of the zinc-coated steel at 450–590°C (840–1100°F) immediately after the steel exits the molten zinc bath. This additional heating allows iron from the substrate to diffuse into the coating. Due to the diffusion of iron and alloying with zinc, the final coating contains around 90% zinc and 10% iron. Due to the alloying of zinc in the coating with diffused iron, there is no free zinc present in the galvanized coating. HDGA coatings contain less aluminum than HDGI coatings, about 0.15 to 0.4 wt-%.

One of the methods by which the coatings are applied to the steel sheet surface is through a process called hot dipping. In this process, continuous coils of steel sheet are pulled at a controlled speed through a bath containing molten zinc. The zinc reacts with the steel and forms a bond. The excess liquid metal sticking on the sheet surface as it exits the bath is wiped off using a gas wiping process and controlled coating weight or thickness per unit area is achieved.

It is reported in the literature that in resistance spot welding of steels with HDGA and HDGI coatings, different electrode life behaviors were seen. For example, Howe and Chen stated that steels with HDGA coatings showed superior electrode lives compared to steels with HDGI coatings (Ref. 2). It is reported that the aluminum content of the coating is the most significant factor affecting electrode life (endurance limit) of HDGI coated sheet steels (Refs. 2–7). Studies of the electrode wear mechanisms in HDGI coatings have shown several possible mechanisms for this accelerated electrode wear.

The effect of the coating type on the spot welding behavior of various aluminum-killed drawing quality steels has

## KEYWORDS

Dual-Phase Steel,  
Resistance Spot Welding  
Current Range  
Weld Tensile Strength  
Hot-Dipped Coatings  
Contact Resistance  
Microhardness Profiles  
GDIS Spectrometer  
Interfacial fractures

M. TUMULURU is with the Research and Technology Center, United States Steel Corp., Munhall, Pa.

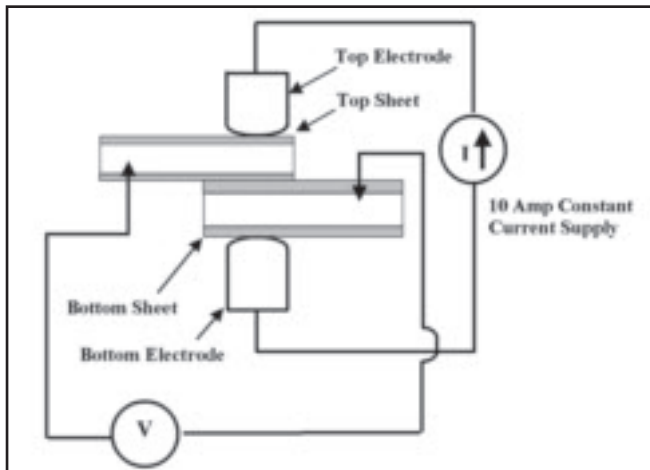


Fig. 1 — Sketch showing the setup used for making the surface resistance measurements. The hatched regions on the sheets represent the coating on the sheet samples.

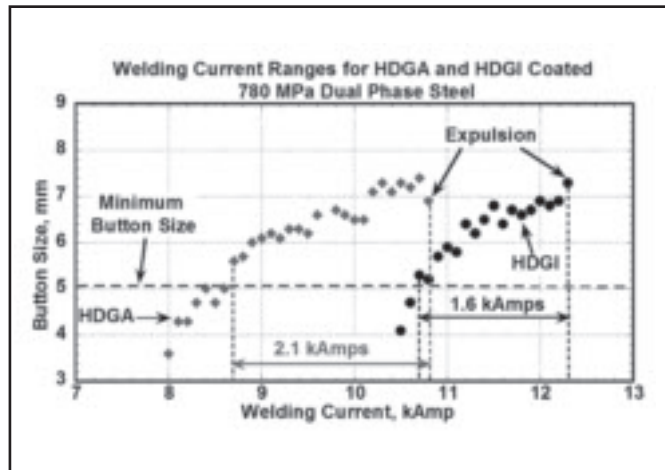


Fig. 2 — Plot of welding current ranges for HDGA and HDGI coated steels.

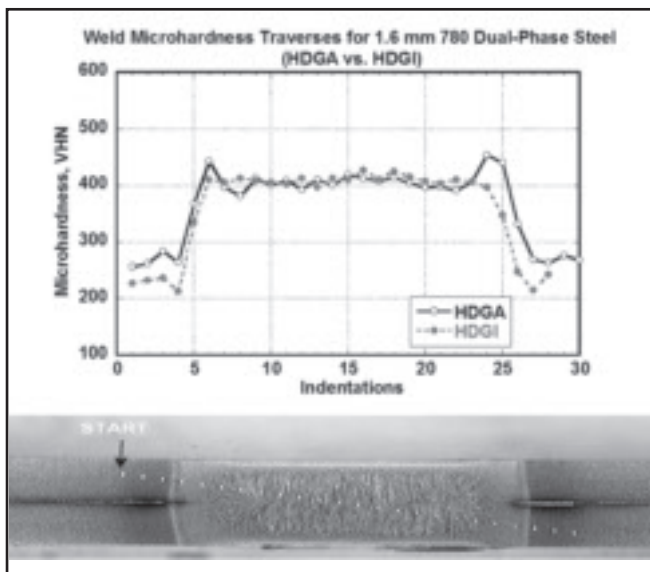


Fig. 3 — Weld microhardness traverses for HDGI and HDGA coated steels and a cross-sectional view of a weld with HDGI coating showing the hardness indentations.

been reported previously. The coating types examined were HDGA and HDGI and electrogalvanized coatings (Refs. 8, 9). It was shown that the HDGA coating had a wider current lobe than the HDGI

coating (Ref. 9). However, Eagar and Gedeon concluded that HDGI material with a very thin Fe-Zn alloy layer have a wider acceptable current range (Ref. 10). They attributed the smaller weld lobe for the HDGA coating to its discontinuous structure and morphology. The effects of the coatings on weld lobes or weld strength for the new advanced high-strength steels, such as the dual-phase steels, have not previously been reported. Because of the higher alloying content of the dual-phase steels compared to low-strength steels (300 MPa), their bulk resistivity is expected to be higher. As a result, these steels require different welding parameters compared to low-strength steels. Therefore, an examination was undertaken to study the effect of HDGI and

HDGA coatings on current ranges and weld tensile strengths for a 780 MPa dual-phase steel.

HDGA coatings on current ranges and weld tensile strengths for a 780 MPa dual-phase steel.

### Materials And Experimental Procedure

In the present study, two different coils of 780 MPa dual-phase steel, one coated with HDGI and the other coated with HDGA, were used. Both coils came from the same heat of steel that was melted, hot and cold rolled at United States Steel Corp. — Gary Works and coated subsequently at PRO-TEC Coating Co., Leipsic, Ohio. Both of the dual-phase steel coils were 1.6 mm thick. All weld testing was carried out on samples in the as-received condition without any cleaning of the mill oil used prior to shipping the coils. Nominally, the steel contains about 0.10 to 0.14 wt-% carbon and is generally alloyed with various amounts of manganese, chromium, and molybdenum to achieve the required tensile strength. The nominal coating weights for the coils used were 70/70 g/m<sup>2</sup> (70 g/m<sup>2</sup> on each side) for the HDGI and 42/42 g/m<sup>2</sup> for the HDGA coating. These coating weights are typical

Table 1 — Welding Equipment Details

Welding machine manufacturer	Taylor Winfield Corp.
Welding machine type	Pedestal type, alternating current
Welding machine transformer	100 kVA
Welding controller	TruAmp IV (constant current type)
Electrode coolant water temperature	21°C
Tip cooling	3.7 L/min (1 gal/min)

Table 2 — Weld Schedules Used for Current Range Test and Weld Tensile Sample Preparation

Electrode material	RWMA Class II (Cu-Cr)
Electrode face diameter, mm	7.0
Electrode tip geometry	Truncated Cone
Electrode force, kN	6.2
Squeeze time, cycles	80
Weld time, cycles	18
Hold time, Cycles	10
Preheating	None
Postheating	None

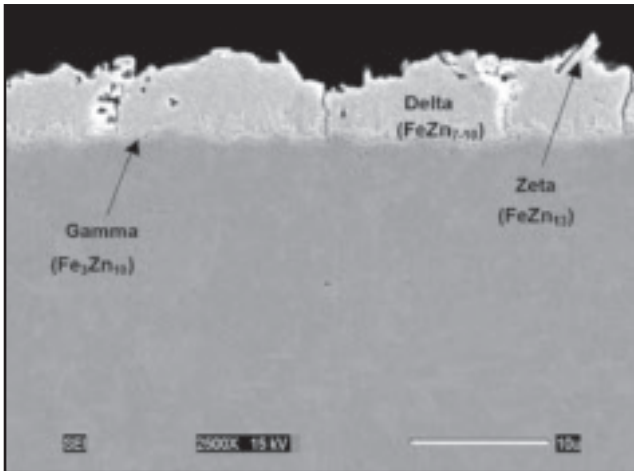
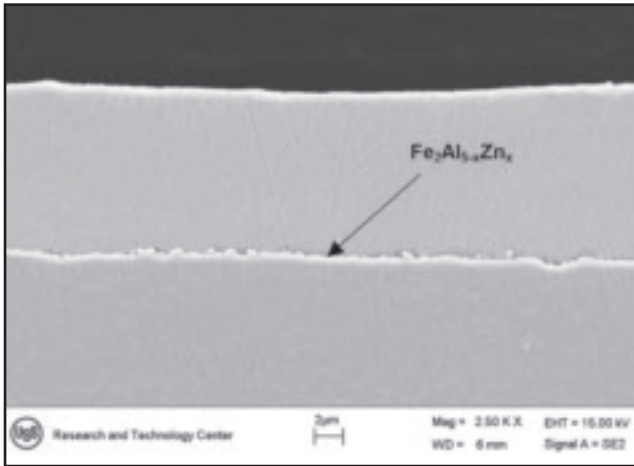


Fig. 4 — Scanning electron microscope sectional views of HDGI (top) and HDGA coatings (bottom). Various constituents in the coatings are marked in the micrographs.

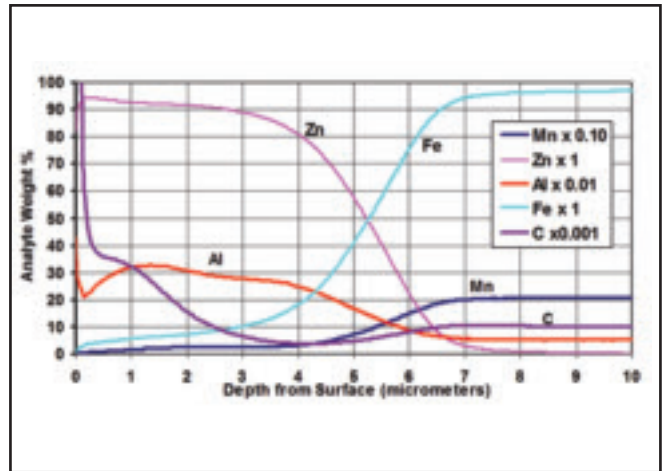
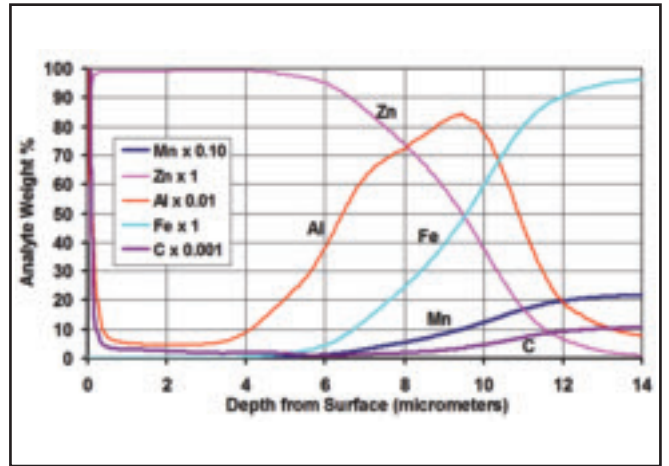


Fig. 5 — Concentration depth profiles from the coating surface obtained by GDS for HDGI coating (above) and HDGA coating (below).

of current commercial automotive use. Due to powdering that galvanneal coatings can exhibit, coating weights are generally restricted, and 42/42 g/m<sup>2</sup> is considered typical in automotive applications.

Two different tests were done to evaluate the effect of the coatings on the welding behavior of the steels. These were the determination of the welding current range and weld shear and cross-tension strength. The tests were conducted first on samples from the HDGA coated steel and then re-

peated on the HDGI coated steel. A brief explanation of the tests and the methods follow. The details of the welding equipment used in this study are provided in Table 1. All of the weld testing was conducted with a pedestal-type Taylor Winfield welding machine using alternating current. The weld schedules used for the current range tests and for making the weld tensile test samples are shown in Table 2.

The current range is the difference between the welding current required to pro-

duce a minimum button size ( $I_{min}$ ) and the current that causes expulsion of weld metal ( $I_{max}$ ). In this study the minimum button size was defined as  $4\sqrt{t}$ , where  $t$  is the nominal sheet thickness. The use of  $4\sqrt{t}$  as the minimum button diameter, where  $t$  is the nominal sheet thickness, is generally used to define the useful current range in the automotive and steel industries. The current range is useful because it provides the range of welding currents over which welds of acceptable size can be produced.

Prior to determining the current range, the electrode tips were conditioned by making 250 welds on flat panels. Current ranges were then determined by first determining the lowest welding current that produced the minimum acceptable button size. Then, the current was gradually increased until weld metal expulsion resulted. The procedure to determine current range is described in detail in Ref. 11.

Weld shear-tension and cross-tension tests were conducted per Ref. 11. The cur-

Table 3 — Weld Shear and Cross-Tension Test Results

Coating	Welding Current, kAmps	Average Shear-Tension Strength, Newtons	Average Cross-Tension Strength, Newtons
HDGA	10.3	23800 (6.9-mm button) Full-Button Pullouts	10200 (6.6-mm button) Full-Button Pullouts
HDGI	11.7	25600 (7.0-mm nuggets) Interfacial Fractures	12300 (6.3 mm Button) Full-Button Pullouts

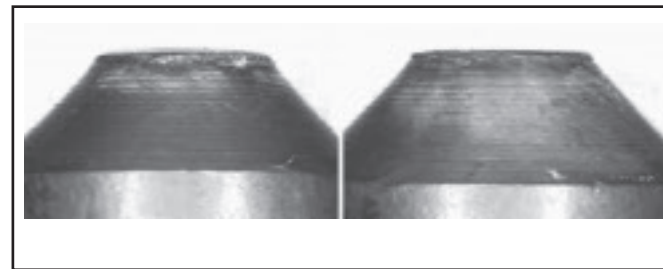
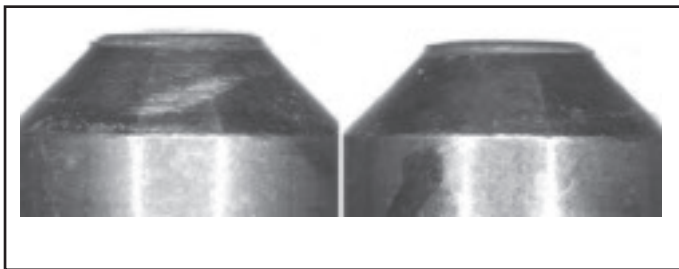


Fig. 6 — Top (left) and bottom (right) electrodes used for the current range determination for HDGA coated steel.

Fig. 7 — Top (left) and bottom (right) electrodes used for the current range determination for HDGI coated steel.

rent required to produce a button size equal to or 90% of the face diameter of the electrode tip used was determined. This was done using the highest current possible without causing expulsion in the samples. If expulsion occurs, the loss of weld metal can adversely affect the tensile strength. The welding current required to produce the tensile samples was determined separately for HDGA and HDGI coated steels.

The welding conditions chosen for this test are typical for the thickness of the material being welded and are considered to be within the capability of the welding equipment currently used in the automotive assembly plants. A weld time of 18 cycles was used both for the current range determination and to prepare weld shear-tension and cross-tension test samples. These two tests were done using a hold time of 10 cycles.

The electrode details were the same for both the tests done. An electrode force of 6.2 kN (1400 lbf) was used and was chosen based on an internal weld schedule optimization study done earlier.

Microhardness traverses were determined at room temperature using a Vickers hardness tester. A force of 1000 g (9.8 N) was used for the microhardness measurements. The hardness indentations were spaced 0.4 mm apart. The microhardness traverses were done on a diagonal to cover as much area in the weld and heat-affected zones as possible. Weld microstructures were examined using both an optical microscope and a scanning electron microscope (SEM). After completion of the current range determination, both the top and bottom electrodes were examined using a SEM.

Cross sections of HDGI and HDGA coated samples were prepared and examined using a SEM. Composition depth profiles of the coatings were obtained using a Leco GDS-750A glow-discharge optical emission spectrometer (GDS or GDOES). The principle used in GDS is that an electric discharge is created in a

low-pressure argon atmosphere. By applying a voltage, argon atoms are ionized and accelerated toward the sample surface to create an ionic bombardment. This ionic bombardment causes the sample to eject atoms (sputter). The ejected atoms collide with ions and create a mechanical energy, which excites the atoms. When the excited atoms return to the ground state, they emit light at a characteristic wavelength. The light emitted by the sample is amplified and passed into a spectrometer. The spectrometer then quantifies the spectral lines based on the wavelength and intensity. Matrix-matched standards are used to calibrate GDS depth profiles and intensity readings. The nonthermal nature of the process makes analysis of even low melting elements easy.

The samples used for the GDS analysis were 2 cm in diameter. The sputter typically produces an analysis area of 4 mm<sup>2</sup>. Concentration depth profiles were performed continuously from one tenth of a nanometer to more than several micrometers in depth, thus covering the areas from the coating surface to the coating-steel substrate interface. Depending on the element analyzed, the precision involved in the analyses is  $\pm 10$  parts per million (ppm).

Contact resistance measurements were made both on the HDGA and HDGI coated samples using a surface resistance analyzer made by C. B. Smith Co. of Placerville, Calif. The setup for making the contact resistance measurements is shown in Fig. 1. Copper probes 12 mm in diameter with a spherical radius of 100 mm were used to obtain the measurements. The contact area of the probes as measured from carbon imprints was 20 mm<sup>2</sup>. Coupons 1 in. by 4 in. were cut from the as-received material. No cleaning was performed on the coupons prior to making the measurements. The test coupons were held under the electrodes under an applied force. The resistance at the faying surfaces was measured as a function of the applied force, which was varied from

667–3780 N. Due to the limitation of the equipment used, force beyond 3780 N could not be obtained. The resistance measured is the sum of the resistivities of the two coatings that are in contact with each other at the faying surface and the surface resistance at the faying surface. In the range of 0 to 150 micro ohms, the precision involved in the measurements was  $\pm 8$  micro ohms.

After welding, the welding electrodes used were examined in a SEM equipped with an energy-dispersive x-ray spectrometer (EDS). Electrode profiles were examined to check for any damage or mushrooming due to the high electrode force used. The electrode tip surfaces were examined to check for any material transfer as well as pitting or erosion.

## Results

The results of the tests to determine welding current ranges for HDGA and HDGI coated steels are shown in Fig. 2. The minimum button diameter line in Fig. 2 is drawn at 5.1 mm and represents a weld button size of  $4\sqrt{t}$ , where  $t$  is the nominal sheet thickness. From Fig. 2 it can be seen that the HDGA coated steel welded at a lower current compared to HDGI coated steel (e.g., 8.7 kA vs. 10.7 kA to obtain the minimum button size). In fact, the weld current that produced expulsion in the HDGA coated steel was only 100 A more than the current that produced the minimum button size in HDGI coated steel. It should be noted that the current range of 1.6 kA obtained on the HDGI coated steels is considered sufficiently wide for automotive applications and should not be an issue for consideration of its use.

The results of the weld shear-tension and cross-tension tests are shown in Table 3. Also shown in Table 3 are the average button sizes measured on the tensile test samples after the tests and the nature of the test sample failure mode. The tensile strength shown in Table 3 represents the load to failure and is based on an average

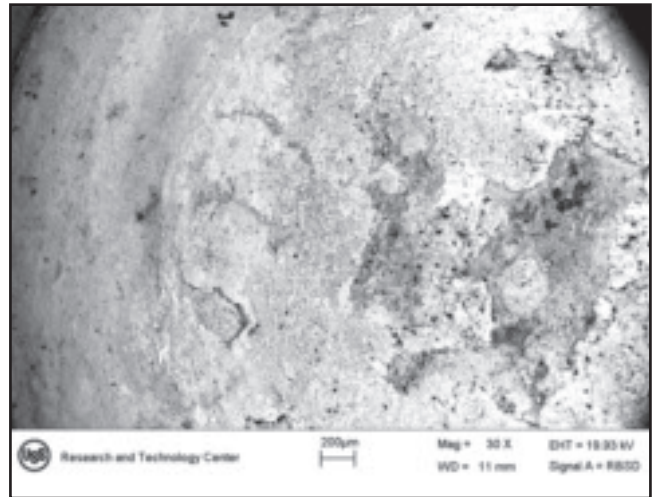
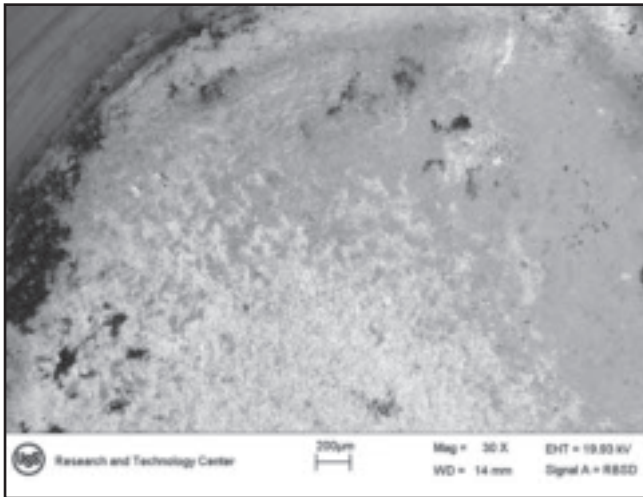


Fig. 8 — SEM view (top) and EDS spectrum from the white film on the faying surface of the electrode used for HDGI steel.

Fig. 9 — SEM view (top) and EDS spectrum from the faying surface of the electrode used for welding of HDGA steel.

of five tests in each case. The microhardness traverses for both the HDGI and HDGA versions of the steel are shown in Fig. 3. This figure shows that the hardness traverses and average peak hardness were similar for the welds with HDGI and HDGA coatings.

Cross-sectional views of both HDGI and HDGA coatings are shown in Fig. 4. The HDGI coating is predominately pure zinc and is intended to provide galvanic protection to the steel substrate. The HDGI coating bath contains anywhere from 0.15 to 0.25% aluminum that reacts with the steel substrate to produce a very thin, flexible Fe-Al-Zn alloy layer at the interface between the steel substrate and the zinc coating. This is believed to provide for a 100% coating coverage to the strip surface and adhesion between the steel and the galvanize coating. The thickness of the Fe-Al-Zn alloy layer is controlled mainly by the aluminum additions to the coating bath, strip and coating bath temperatures and galvanizing strip line speed. The bulk HDGI coating typically contains from about 0.30 to 0.60% Al. The cross-sectional view of a HDGI coating etched to reveal the intermetallic alloy inhibition layer ( $Fe_2Al_{5-x}Zn_x$ ) is shown in Fig. 4. The

overall HDGI coating thickness is around 11 microns.

Several of the properties of both HDGI and HDGA, and hence their effect on welding behavior, can be understood by examining the distribution of various elements from the surface of the coating to the steel substrate. The GDS profiles obtained for the two types of coatings studied are shown in Fig. 5. Because the amounts of various elements present across the coatings are significantly different, multiplication factors were used to calculate the amounts present at any given location. This was done to present a comprehensive view of the distribution of various elements across the depth of coatings in one plot. To calculate the content of any element in weight percent at any given point along the depth of the coating, the amount of that element read from the y-axis should be multiplied by the factor noted for that element in the legend. For example, the amount of aluminum present in the HDGA coating at a depth of 2  $\mu m$  is 0.30 wt-%. This was obtained by the amount of aluminum present at 2  $\mu m$  (which is 30) with a multiplication factor of 0.01 for aluminum. Similarly, the amount of zinc at 4- $\mu m$  depth in the

HDGI coating is calculated by reading its content on the y-axis (which is 100), which is multiplied by the multiplication factor for zinc (which is 1), and this gives 100% by weight percent.

The HDGA coating consists of a multiphase intermetallic Zn-Fe<sub>10</sub> alloy structure containing typically about 8 to 12% iron. The HDGA coating is harder and brittle compared to the HDGI coating. The HDGA structure typically consists of mainly delta<sub>1</sub> ( $\delta_1$ ) Fe-Zn alloy phase, a thin brittle gamma ( $\Gamma$ ) phase (Fe<sub>3</sub>Zn<sub>10</sub>) at the steel-coating interface, which has higher iron content. The coating may also contain some zeta ( $\zeta$ ) phase (FeZn<sub>13</sub>) at the surface. The surface of HDGA coatings is characterized by Fe-Zn alloy crystals and micro-craters. It is normal for HDGA coatings to have microcracks as-produced, more frequent and larger after temper rolling and after stamping. The coating bath for HDGA typically contains about 0.12 to 0.14% dissolved aluminum. The bulk coating averages about 0.15 to 0.40% aluminum. From Fig. 4, the average HDGA coating thickness is around 6 microns.

Figure 5 indicates that the HDGI coating is very rich in aluminum and shows nearly 100% aluminum on the coating sur-

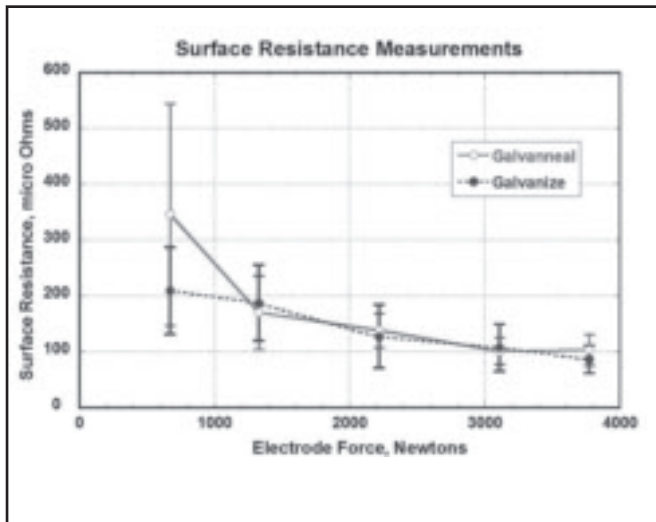


Fig. 10 — Plot of contact resistance as a function of electrode force.

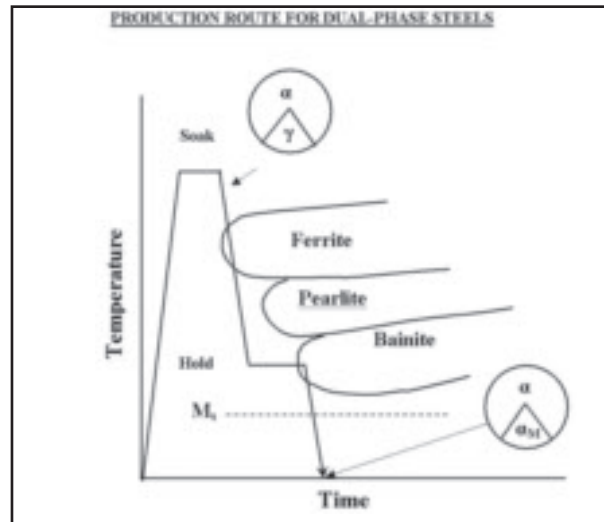


Fig. 11 — A schematic of the production route for dual-phase steels.  $M_s$  represents the martensite-start temperature.

face. The aluminum layer appeared to be very thin and is probably around 10 nanometers. Due to its high affinity for oxygen, the surface aluminum exists as aluminum oxide. The aluminum content then rapidly decreased to about 0.05 to 0.1% and did not show an increase until the intermetallic alloy inhibition layer ( $Fe_2Al_{5-x}Zn_x$ ) is reached. The intermetallic alloy layer ( $Fe_2Al_{5-x}Zn_x$ ) is about 100 nm thick. It averaged about 45% aluminum.

Figures 6 and 7 show the electrode profiles. It appeared from these figures that the electrodes did not show any detectable mushrooming despite the use of a high electrode force. From Figs. 8 and 9, which show the SEM views of the electrode tip surfaces, it can be seen that the electrode used for welding of HDGI samples showed a whitish-looking film on the electrode tip surface. EDS analysis of the film showed the presence of aluminum. This indicates the transfer of the alumina from the coating surface to that of the electrode tip. Because the alumina layer is only a few nanometers thick, the zinc and the copper peaks in this spectrum are believed to be from the background. During EDS analysis, the electron beam broadens and for thin material or films, a part of the spectrum is collected from the background.

The results of the surface resistance tests are shown in Fig. 10. The results showed that there seems to be no detectable difference in the surface resistance between the HDGA and the HDGI coatings.

## Discussion

### Microstructural Evolution

To understand the welding behavior, it

is helpful to examine the microstructure of the base material and how it is achieved. Figure 11 shows a schematic representation of the heat treatment steps involved in dual-phase steel production through a continuous galvanizing line. The steel is typically annealed intercritically to form between 25 and 50% austenite and cooled in such a manner to avoid the formation of pearlite and bainite (Ref. 12). For processing in a continuous galvanizing line, a hold zone typically exists at about 470°C, followed by immersion in the coating bath that is typically at 460° to 465°C. To achieve a minimum tensile strength of 780 MPa, dual-phase steels typically contain about 20 to 30% martensite in a soft ferrite matrix — Fig. 12. The steel is alloyed in such a way that it does not form an appreciable amount of bainite during the holding time.

Microscopic examination of the welds showed the presence of martensite both in the weld and the heat-affected zones — Fig. 13. In resistance spot welding, due to the water cooling of the electrodes, the weld cooling rates are extremely rapid. Spot welds in thickness up to 2 mm typically solidify in less than three to four cycles. It has been shown through modeling that even at 500°C the cooling rates in spot welding were in excess of 1000°C/s (Ref. 13). For steels, the critical cooling rate  $v_c$ , required to achieve martensite in the microstructure, is given by the following equation:

$$\log v_c = 7.42 - 3.13 C - 0.71 Mn - 0.37 Ni - 0.34 Cr - 0.45 Mo \quad (14)$$

For the 780 MPa dual-phase steel used here, the critical rate turns out to be about

240°C/s. Therefore, it is not surprising that a martensitic structure is present both in the weld and the heat-affected zone. An interesting observation is that, even though HDGA steel required lower current to weld and thus had lower heat input, because the weld cooling rates are so high and the critical cooling rate to achieve martensite is comparatively low, the HDGA steel also showed a fully martensitic microstructure in the heat-affected zone. Thus, the lower welding current required to form a nugget in HDGA compared to HDGI did not appear to be an advantage.

An advantage of the use of lower welding current cited often is that it provides longer electrode life and causes less distortion in the base material due to less heating (Refs. 2, 15). However, in automotive manufacturing plants, it is not uncommon to find that electrode tips are dressed after every 30 to 50 welds to maintain weld quality and weld size. Therefore, the longer electrode life offered by the HDGA coating may not be an advantage over that of the HDGI coating.

### Effect of Surface Resistance

In resistance welding, heating of the materials to be joined is realized through  $I^2Rt$ , where  $I$  is the current used for welding,  $R$  is the resistance offered to the passage of current and  $t$  is the time of passing the current. Further, based on a formula developed at this laboratory (Ref. 16), the calculated value of bulk resistivity of the steel was only 24.7 micro ohms-cm and is relatively low when compared to the resistance measured at the faying surfaces. The resistance  $R$  of a conductor is given by

$$R = \rho L/A$$

Where  $\rho$  is the resistivity of the conductor,  $A$  is its cross-sectional area, and  $L$  its length. This means the resistance of a conductor is directly related to its length. From Fig. 4, it is apparent that the thickness of the HDGA coating is almost half that of the HDGI coating. Therefore, it is reasonable to think that the HDGA coating in this case would offer lower resistance. The electrical resistance measurements shown in Fig. 10 indicate that there is no significant difference in the total resistance at the faying surface between the HDGA and the HDGI coatings at higher electrode force. This suggests that the resistivity differences between the coatings may not explain why the coatings required different currents to produce the minimum required weld size. It should be noted that the surface resistance measured is the static not dynamic (changes during welding) resistance. Static response is the controlling factor in the first few cycles of passing the current and thus dictates the current required to initiate heating for welding.

As heat develops at the faying surfaces, the effect of static contact resistance decreases and dynamic resistance takes over. Recent Gleeble studies on mild steel have shown that with a rise in the temperature the dynamic resistance may not always show the same trend. Whether the dynamic resistance increases or decreases during the later stage depends on interplay of various factors such as the electrode pressure and substrate resistivity (Ref. 17). A discussion on the various stages involved in the nugget formation and the contribution of dynamic resistance during nugget development is provided in Ref. 18.

HDGA coating has an irregular surface topography and through-thickness cracks. The irregular topography can cause high current density at the peaks in the coating. Therefore, rapid localized melting of the coating can occur. This can promote early heat development and may need less current to generate further heat for welding. Earlier studies on the effect of surface topography of coatings that are consistent with the present findings found that surface roughness had a significant effect on the welding behavior of steels (Refs. 18, 19). For example, in Ref. 18, the authors examined the effect of surface roughness and reported that the sample that had the roughest surface required the lowest welding current to produce a weld nugget. The authors noted that the surface asperity contact on a rough surface concentrated the current at local spots and promoted early asperity heating and collapse. This, in turn, lowered the welding current for subsequent heat generation to

form the weld nugget.

The GDS results revealed the presence of a thin aluminum layer on the HDGI coating surface. Examination of the electrode tips used for welding of HDGA and HDGI samples showed that the contact surfaces of both the top and bottom electrodes showed the presence of aluminum, more on the HDGI, indicating that some of the surface aluminum was transferred to the electrode contact surface. Aluminum exists as alumina (aluminum oxide). It is known that alumina is a refractory oxide with a melting point of 2072°C. It has poor electrical and thermal conductivity. The presence of alumina on the electrode tip surface when welding HDGI coated steel, therefore, should make it difficult to pass current to the sheets and would require high voltage and current to overcome its poor electrical conductivity.

The presence of alumina on the electrode tip (the tips were conditioned prior to use) requires higher current and voltage to overcome alumina's poor electrical resistance. Although the presence of alumina on the HDGI sheet surface increases the electrical resistance, the welding current has to first overcome the resistance barrier imposed by the presence of alumina on the electrode tip surface. Measurements indicated that the contact resistance between the HDGI and HDGA surfaces was similar and no statistical difference was detected. This indicates that interfacial resistance was lowered by the use of high electrode force. This further means that the effect of the presence of alumina layer on the HDGI sheet-electrode tip surfaces and the sheet interfaces was minimized by the use of high electrode surface and the presence of alumina on the HDGI sheet surfaces did not account for the differences noted in the welding current required for nugget formation. Any heat developed at the electrode tip and sheet top surface alumina layer is conducted away by the water-cooled electrodes and is not useful for welding. However, this alumina layer is also a barrier to overcome for the passage of current. Therefore, the presence of an alumina layer on the electrode tip surface when welding HDGI samples appeared to

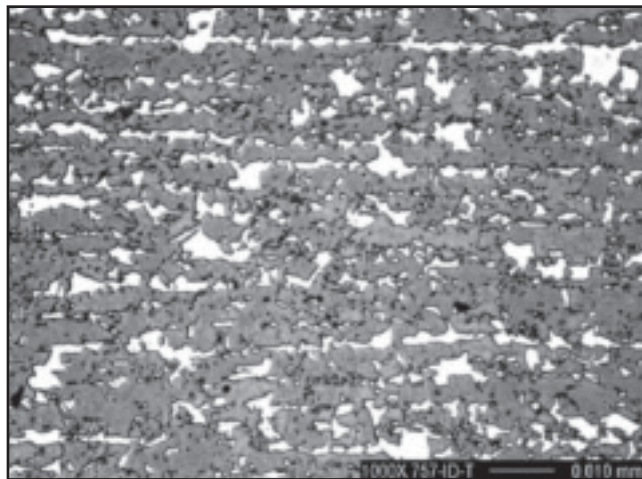


Fig. 12 — Microstructure of 780 MPa minimum tensile strength dual-phase steel. The dark etching areas are ferrite and the white islands are martensite.

be the key factor here and is believed to be the reason for HDGI coated samples to be welded at higher current than HDGA samples.

## Weld Strength

The average load to failure for HDGI welds in the shear-tension test and cross-tension tests was higher compared to the HDGA welds. However, the differences in the tension tests between HDGI and HDGA coated steels are not statistically significant due to the scatter generally seen in the weld tensile tests. This suggests that, as long as the nominal weld sizes produced in the samples are of the same size and are produced without weld metal expulsion, the spot weld tensile strength is independent of the type of coating and is controlled by the substrate properties.

The importance of weld nugget size should be emphasized because the size (or diameter) of the welds controls the weld tensile strength. Studies done at this laboratory on several high-strength steel grades and at various sheet thicknesses have shown a strong dependence of the fracture appearance (or mode) on weld size in spot weld shear-tension tests (Ref. 21). It was found through modeling of actual test results that the failure load for a full-button pullout is given by

$$F_{PO} = 2.25 S_{BM} \cdot d \cdot t$$

where  $S_{BM}$  is the tensile strength of the base metal,  $d$  is the weld diameter, and  $t$  is the sheet thickness. The load to failure and the weld sizes were at the transition between full button pullout to interfacial fractures and, as such, either fracture

mode was possible. The important point here is that, despite different fracture modes seen in HDGA and HDGI, the load to failure was essentially the same. Therefore, fracture mode should not be used as the sole criteria to judge weld integrity in high-strength steels. It was observed that the weld tensile strength in high-strength steels, such as the steel in this study, is more sensitive to the occurrence of expulsion of weld metal compared to low-strength, drawing-quality steels (Ref. 22). Therefore, it is also important to note that welds in tensile test samples should be produced without expulsion because expulsion of weld metal is detrimental to the weld tensile strength as it lowers the effective weld size. With regard to the hardness traverses, the observation that the hardness distribution in the welds between HDGI and HDGA coated steels was similar is not surprising. The weld area hardness is a function of the weld metal microstructure, which in turn, is controlled by the base material composition and the weld cooling rates. The base material used for making both the HDGA and the HDGI coated sheets came from the same heat of material.

#### Coating Selection Considerations:

This study examined the relative welding behavior of 780 MPa steel coated with HDGA and HDGI. The coating weights selected in this study are used by some automotive manufacturers in the industry. Therefore, it should be kept in mind that this study pertains only to the coating weights selected. This study showed that there appears to be no advantage of one coating over the other and that both HDGA and HDGI have a similar welding performance. It may be possible to lower the current required to achieve the minimum button in HDGI by lowering the coating weight to 60/60 g/m<sup>2</sup>. It was shown that a decrease in coating thickness decreased the current required to form a nugget (Ref. 23). This suggests that, once the current required to pass through the electrode tip surface alumina layer is established and the current reaches the sheet surface, a reduction in the HDGI coating thickness lowers the distance the welding current has to travel and thus reduces the subsequent resistance for current passage. However, it is cautioned that this decision to lower the coating thickness should be made only after a careful and independent examination of the effect of lowering the coating weight on the corrosion behavior and other manufacturing considerations.

The aim of this study was to take a comparative look at the welding performance of HDGI and HDGA coatings. However,

other performance attributes of these coatings should also be carefully examined before selecting the type of coating to use. These attributes include, but are not limited to, the corrosion protection offered, formability, and cost. A detailed study on the relative corrosion performance of HDGI and HDGA coatings is provided in Ref. 24. While some auto manufacturers prefer to use galvanized steel, others prefer to use galvanized steel, others prefer to use galvanized steel. A decision to switch the type of coating from one to the other is not a simple one and depends on a wide variety of manufacturing considerations. Some of these considerations include the equipment available for alkaline cleaning prior to painting the surface, the extent of forming involved, and the automobile manufacturer's design and emphasis on the type of corrosion resistance (for example, creep-back corrosion vs. corrosion resistance at paint chips) required.

#### Conclusions

The following conclusions can be reached based on the study conducted to examine the differences between HDGI and HDGA-coated 780-MPa dual-phase steels:

1. The welding behavior of 780 MPa dual-phase steel coated with 70/70 g/m<sup>2</sup> HDGI and 42/42 g/m<sup>2</sup> HDGA, coating weights that are currently used in the automotive industry, was similar. One difference noted between the two coatings was that HDGA required lower welding current to form the minimum nugget size. This may not be an advantage in the industry given the current practice of frequent electrode tip dressing.

2. Welding current range for HDGA was wider than for HDGI. However, the welding current range of 1.6 kA obtained for HDGI coated steel is considered sufficiently wide for automotive applications and should not be an issue for considera-

tion of its use.

3. The type of coating had no effect on the weld shear-tension or cross-tension strength. The weld strength is controlled by the steel substrate.

4. The HDGI coated steel showed interfacial fractures in shear-tension but not the HDGA coated steel. The reason for this behavior is believed to be that the load to failure and the weld sizes were such that either full button pullout or interfacial fractures were possible. The fracture mode is not considered significant because the load-bearing ability of the welds remained unchanged between the two fracture modes.

#### Disclaimer

The material in this paper is intended for general information only. Any use of this material in relation to any specific ap-



Fig. 13 — SEM views of the weld metal (top) and heat-affected zone (bottom) microstructures. The weld showed a completely martensitic structure. Isolated areas of ferrite and bainite were seen in the heat-affected zone. Nital-Picral etch.

plication should be based on independent examination and verification of its unrestricted availability for such use and a determination of suitability for the application by professionally qualified personnel. No license under any United States Steel Corp. patents or other proprietary interest is implied by the publication of this paper. Those making use of or relying upon the material assume all risks and liability arising from such use or reliance.

## References

1. Engl, B. 1997. Automotive body materials. *IBEC 1997*.
2. Howe, P., and Chen, C. C. 1999. The effects of coating composition, substrate, and welding machine on the resistance spot welding behavior of hot-dip galvanized and galvanized sheet steels. *IBEC 1999*.
3. Goodman, S. R., and Domis, W. 1982. Effects of carbon, phosphorus, and sulfur content on the tensile properties of high-strength cold-rolled sheet. SAE Paper 820280, Detroit, Mich.
4. Dickinson, D. W. 1981. Welding in the automotive industry. AISI Research Report SG81-5, August.
5. Matsuda, H. et al. 1998. Effect of aluminum on spot weldability of hot-dipped galvanized and galvanized steel sheets. Paper 1-5 of *AWS Sheet Metal Welding Conference VIII Proceedings*, October 14, 1998.
6. Auto/Steel Partnership Welding Task Force, Electrode Wear Mechanisms Project. 1994. Mechanisms of electrode wear during spot welding hot-dipped galvanized steel. A/SP Technical Report, March 1994.
7. Gugel, M. D., White, C. L., Kimchi, M., and Pickett, K. 1994. The effect of aluminum content in HDG coating on the wear of RSW electrodes. Paper D3 of *AWS Sheet Metal Welding Conference VI Proceedings*, October.
8. Gould, J. E., and Peterson, W. E. 1988. A detailed examination of weldability lobes for a range of zinc-coated steels. SAE Technical Paper 880279, Detroit, Mich., February 1988.
9. Natale, T. V. 1986. A comparison of the resistance spot weldability of hot-dip and electrogalvanized sheet steels. SAE Technical Paper 860435, Detroit, Mich.
10. Gedeon, S. A., and Eagar, T. W. 1986. Resistance spot welding of galvanized steel: Part I. Material Variations and Process Modifications, *Met Trans. A*, Vol. 17B, pp. 879-885.
11. D8.9M-2002, *Recommended Practices For Test Methods for Evaluating the Resistance Spot Welding Behavior of Automotive Sheet Steel Materials*. Miami, Fla.: American Welding Society.
12. Hassani, F., and Yue. S. 1999. A comparison of bainitic TRIP and dual phase microstructures. *41st MWSP Conference Proceedings*, ISS, Vol. XXXVII.
13. Li, M. V., Dong, D., and Kimchi, M. Modeling and analysis of microstructure development in resistance spot welds of high-strength steels. SAE Technical Paper 982278, SAE International, Warrendale, Pa.
14. Easterling, K. E. 1993. Modelling the weld thermal cycle and transformation behavior in the heat-affected zone. *Mathematical Modelling of Weld Phenomena*, Eds. H. Cerjak and K. E. Easterling. The Institute of Materials.
15. Howe, P., and Kelley, S. C. 1988. A comparison of the resistance spot weldability of bare, hot-dipped, galvanized and electrogalvanized sheet steels. SAE Technical Paper 880280, Detroit, Mich.
16. Ludwigson, D. C., and Schwerer, E. C. 1971. *Metallurgical Transactions*, Vol. 2, December.
17. Song, Q., Zhang, W., and Bay, N. 2005. An experimental study determines the electrical contact resistance in welding. *Welding Journal* 84(5): 73-s to 76-s.
18. Dickinson, D. W., and Natale T. V. 1982. The effect of sheet surface on spot weldability. *Technological Impact of Surfaces*. ASM International, Materials Park, Ohio, pp. 229-249.
19. Fostini, R. V., and Dilay, W. 1982. The effect of surface coating on the weldability of HSLA Steels. *Technological Impact of Surfaces*. ASM International, Materials Park, Ohio, pp. 251-293.
20. Natale, T. V. 1984. Resistance spot weldability of thin gauge zinc coated sheet steel. *Proceedings of the AWS Sheet Metal Welding Conference*, October 1984.
21. Radakovic, D. J., and Tumuluru, M. Factors influencing fracture mode in resistance spot weld shear-tension testing of advanced high strength steels. Paper presented at FABTECH International & AWS Welding Show, 2006, Atlanta, Ga.
22. M. D. Tumuluru, Internal U.S. Steel report.
23. Mathieu, S., and Patou, P. 1985. Zinc coating influence on spot-weldability of hot-dipped galvanized steel sheets. SAE technical paper 850273, Detroit, Mich.
24. Simko, M., Roudabush, L. A., and Ban, S. 1995. Corrosion behavior of zinc and zinc-alloy coated sheets for automotive applications: An overview and initial results. Paper presented at Galvatech '95, Sept 17-21, Chicago, Ill.

## Want to be a Welding Journal Advertiser?

For information, contact  
Rob Saltzstein at  
(800) 443-9353, ext. 243,  
or via e-mail at  
[salty@aws.org](mailto:salty@aws.org).

## An Important Event on Its Way?

Send information on upcoming events to the Welding Journal Dept., 550 NW LeJeune Rd., Miami, FL 33126. Items can also be sent via FAX to (305) 443-7404 or by e-mail to [woodward@aws.org](mailto:woodward@aws.org).